Transmitter Identification —Experimental Techniques and Results—

Tsutomu SUGIYAMA, Masaaki SHIBUKI, Ken IWASAKI, and Takayuki HIRANO

We delineated the transient response patterns of several different radio transmitters in order to determine the patterns most useful in the development of a transmitter identification system. Using a high-speed data acquisition system, we first obtained rise and fall data for various transient response patterns that were produced by six different FM radio transmitters when the press-to-talk buttons were swicthed on and off. We next evaluated the effect of these transient patterns on the time domain and time-frequency spectrograms by measuring the changes in the receiver input level at Pin = -120 dBm and SNR = 7.2 dB obtained from three different bandwidths : 250, 50, and 12 kHz. Similarly, spectrogram analysis was used to obtain information about the relationship between bandwidth and noise. Comparison of the spectrogram patterns obtained in both laboratory and field experiments independently corrobrated our results. However, the transient patterns in the time domain could not be used because of extensive distortion related to noise and interference from neighboring radio stations. These results suggest that spectrogram analysis of transient reponse patterns may be the most effective way to secure reliable identification of the FM radio transmitters.

Keywords
Radio transmitter identification, Spectrogram pattern, Wigner-distribution

1 Introduction

Local Bureaus of Telecommunications confirmed that there were approximately 36,000 illegal radio stations in 1997, approximately 45,000 in 1998 and approximately 37,000 in 1999[1]. Illegal stations cause problems by leading to interference and jamming of important or general-operational radio communications. Adequate measures must be taken against such problems. We conducted a study to identify press-to-talk transmitters by analyzing their transient-response characteristics at the time of the transmitters are turned on and off[2]. A previous study reported that a transient response lasted for several μs to several hundreds of ms[3]. Insufficient reports were available regarding detailed descriptions of the reproducibility, stability, and effect (on the environment) of a transient-response duration, thus it was difficult to develop an effective procedure for identifying radio transmitters. In the earlier part of this report, in order to determine the general characteristics and tendencies of the transient-response duration, we applied the saturation voltage to normalize an amplitude envelope at the time of a signal rise[4]. We also examined the effects of variations in power voltage and ambient temperature on performance in the identification of radio transmitters. In the latter part of this report, we compare the results of the above-mentioned indoor experiment with the experimental results obtained using an antenna, to determine the effectiveness of the present system with various types of transmitters.

In the field experiment, we qualitatively and quantitatively evaluated 1) a change in the input level (Pin) and 2) its effects on an amplitude envelope waveform and spectrogram at the time of a rise in the time domain. The evaluation of the spectrogram was compared with that made in the indoor experiment. This comparison revealed that the patterns of a spectrogram with characteristic values of -120 dBm and SNR = 7.2 dB agreed in the indoor and field experiments. Therefore, such patterns may be applied to the identification of radio transmitters.

2 Indoor experiment

In this indoor experiment, we used the same high-speed data-acquisition system in the previous report that described the configuration of the system, connection to signals, and the installation. Twenty-four radio transmitters made by three manufacturers were examined in this experiment, divided into 6 models. In this report, α indicates a 144-MHz band, while β indicates a 430-MHz band. 'A,' 'B,' and 'C' are manufacturers. For details, refer to Appendix 1 for the specifications of the transmitters.

Fig.1 shows typical amplitude envelope waveforms at the time of a rise for 6 models of the three manufacturers. The vertical axis indicates the amplitude in units of mV, while the horizontal axis indicates the duration of time in units of ms. Manufacturer A, shown at the top of this figure, had a pulse-like waveform that converged in a short period before a major rise appeared. At the major rise, the waveform overshot and then slowly attenuated, reaching a constant level. After overshooting, Manufacturer B's waveform gradually attenuated and converged at a constant level. Unlike A, B had no pulse-like waveform, overshot for a longer time, and had a round pattern. Manufacturer C's waveform did not overshoot, increased slowly, and saturated after an extended period. Thus, amplitude envelope waveforms differed by transmitter model.

Fig.2 shows falling waveforms. All transmitters had their signal levels cut off, greatly reducing the time required for falling. This produced very little of the information necessary to identify transmitters, compared with the use of data for a rise. Therefore, we decided to examine data for a rise in order to identify transmitters.

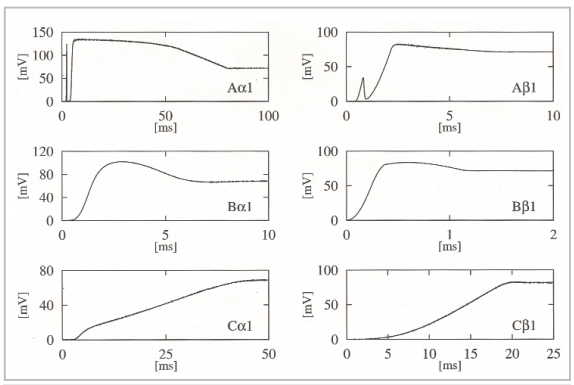

Fig.1 *Amplitude envelope waveforms at the time of a rise*

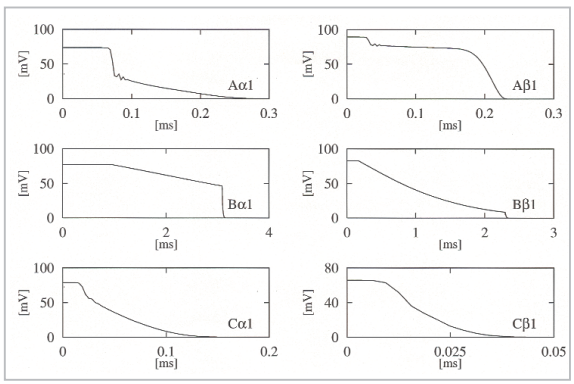

Fig.2 *Amplitude envelope waveforms at the time of falling*

2.1 Processing and evaluation of acquired data

We now know from Fig.1 that amplitude envelope waveforms differed by transmitter manufacturers and model. To process acquired data, we define an inter-threshold time lag, as shown in Fig.3. Assuming the saturation level (V) of the amplitude to be 100, the amplitude voltage (Vs) is normalized every 10% during transition. We refer to the transition process as a "threshold." A time lag between thresholds, Δt, is defined as the time required for the voltage to reach a value of Vs

with the saturation time defined as 0 ms. Fig.4 shows a typical relationship between the time lag and the normalized amplitude voltage. This example is a result obtained from 10 continuous measurements using the 144-MHz band Model 1 of Manufacturer A. The bars in the figure indicate the error ranges around an average. The evaluation of envelope waveforms was conducted in comparison with the indoor-experiment data, and is described below.

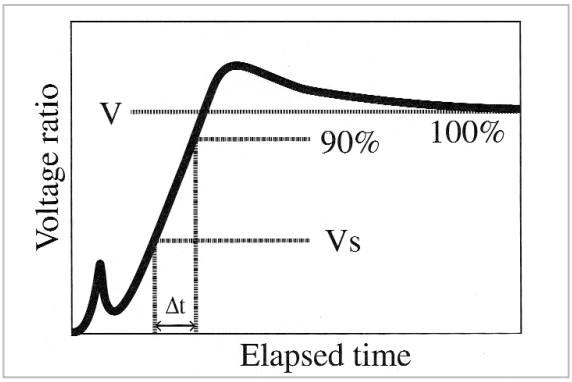

Fig.3 *Definition of inter-threshold time lag*

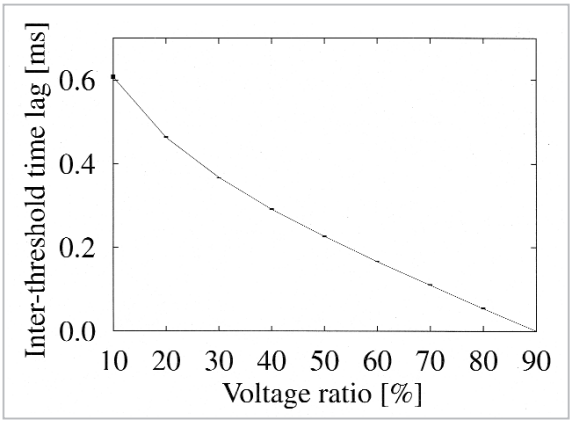

Fig.4 *Plotting of the inter-threshold time lag against normalized voltage*

2.2 Dependence of the time-lag-normalized voltage relationship on the power voltage

Fig.5 shows the measured relationships between the inter-threshold time lag and the normalized voltage at differing power voltages. These results were obtained by averaging the measurements for supply voltages of 15.2 V, 13.8 V, and 12.4 V at a temperature of +25°C. The transmitters were placed in a thermostatic chamber. As can be seen from this figure, the time lag tended to decrease with an increase in the supply voltage. This proved to be common to all of the models we examined. Model α1 of Manufacturer C, however, showed the strongest tendency in this regard.

2.3 Dependence of the time-lag-normalized voltage relationship on the temperature

Fig.6 shows the measured relationships between the inter-threshold time lag and the normalized voltage at differing temperatures. We placed the transmitters in a thermostatic chamber to obtain these results by averaging ten consecutive measurements each at temperatures of +40°C, +25°C, and –10°C. In Fig.6, the vertical bars indicate errors. It was common to the six models of the three manufacturers that, as the set temperature lowered, the inter-threshold time decreased. Most of the models behaved similarly, except that Models α and β of Manufacturer C showed relatively large dependencies. Model β of Manufacturer A showed a large change in voltage of between 10% and 20% at –10°C, due the effect of a pulse-like waveform prior to a rise.

2.4 Difference in the time-lag-normalized voltage relationship among four transmitters of the same model

Fig.7 shows the differences in the time-lag-normalized voltage relationships among four transmitters of the same model. The measurement conditions were a constant temperature of +25°C and power voltage of 13.8 V. The four transmitters in each group behaved similarly, except for Manufacturer A's Model α1. Fig.8 shows the averaged relationships for all models, indicating that there is a good possibility of identifying transmitters based on the significant differences among their six types. As all models of each manufacturer behaved similarly, it may be possible to identify the manufacturer of a transmitter. It may also be possible to distinguish between the different models of one manufacturer. However, it will be difficult to identify trans-

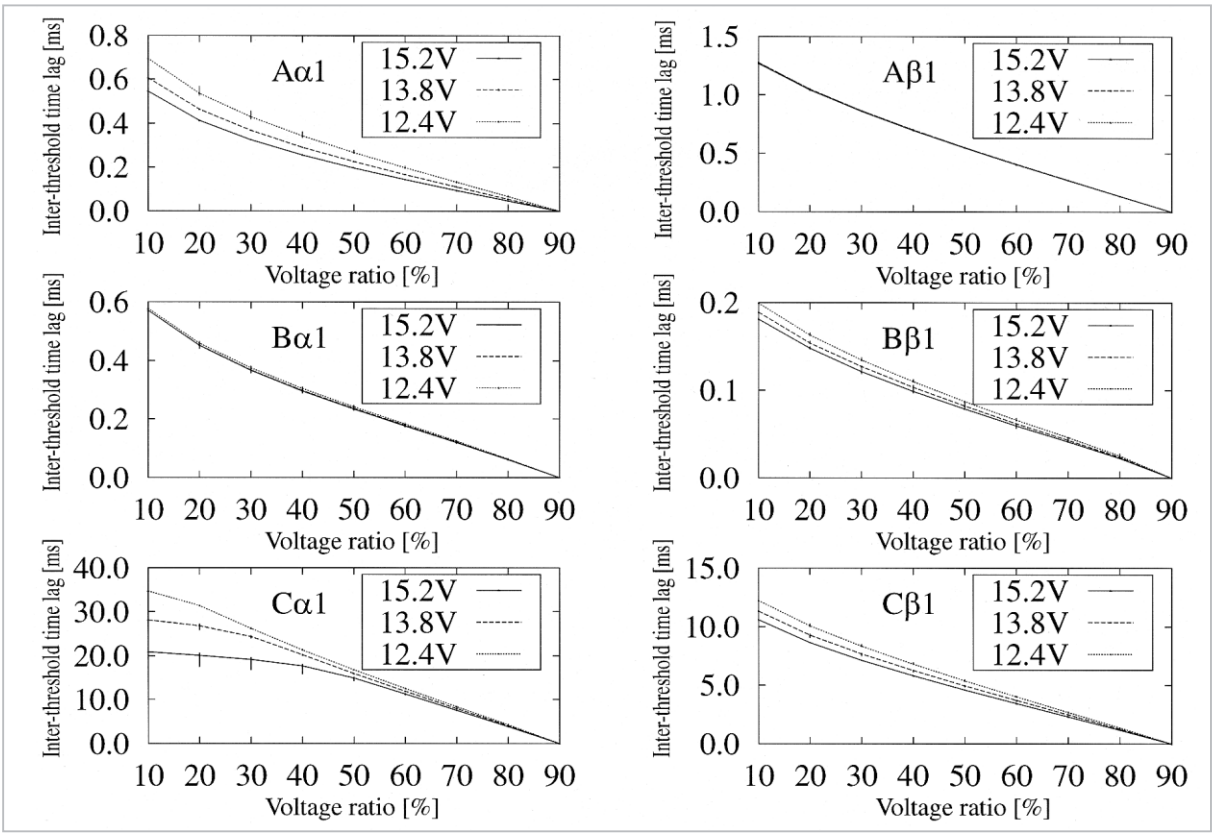

Fig.5 *Dependence of the time-lag-normalized voltage relationship on the power voltage*

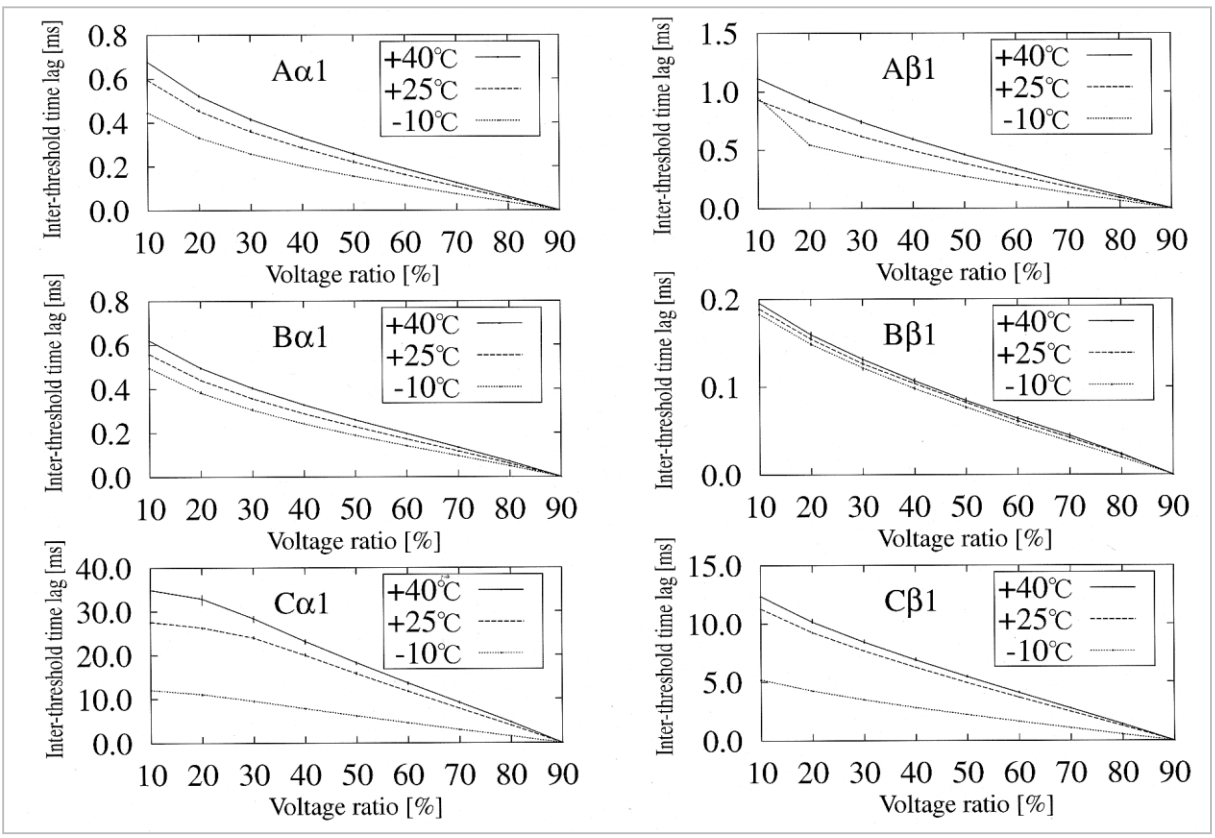

Fig.6 *Dependence of the time-lag-normalized voltage relationship on the temperature*

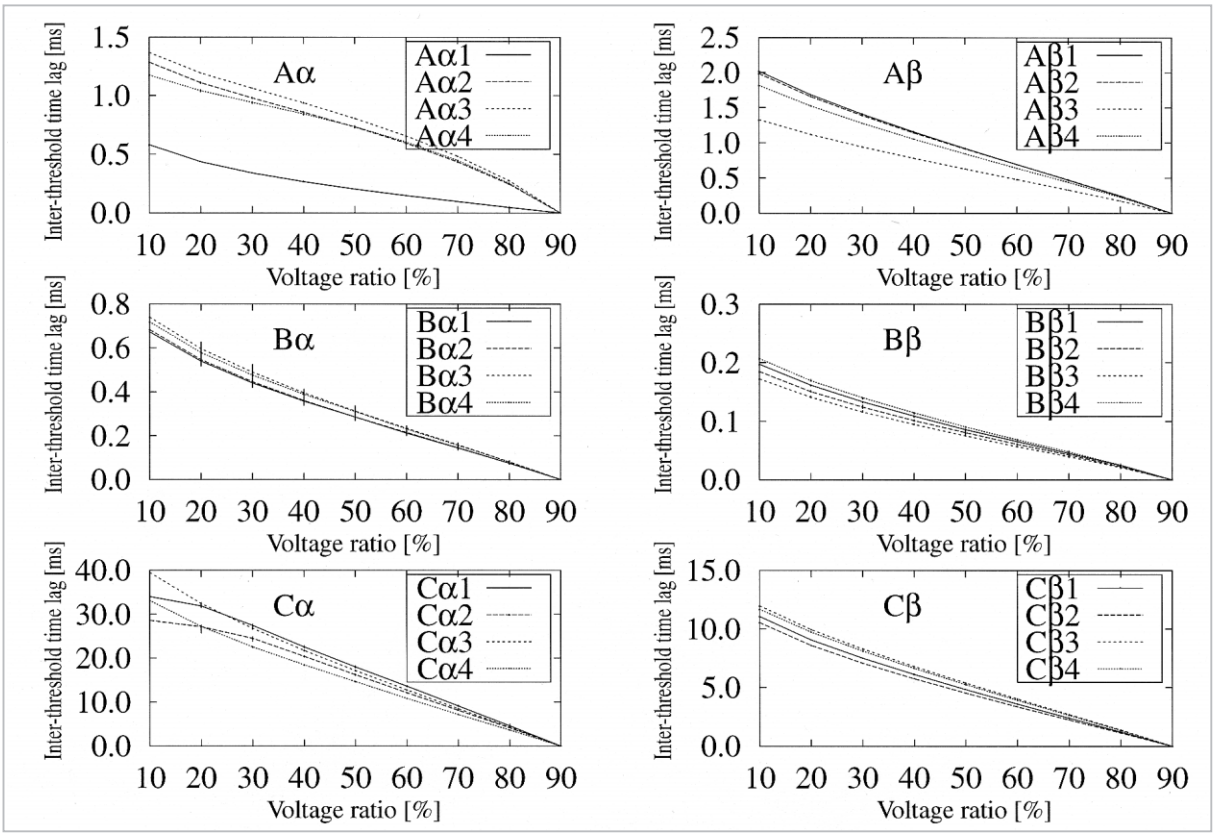

Fig.7 *Difference in the time-lag-normalized voltage relationship among four transmitters of the same model*

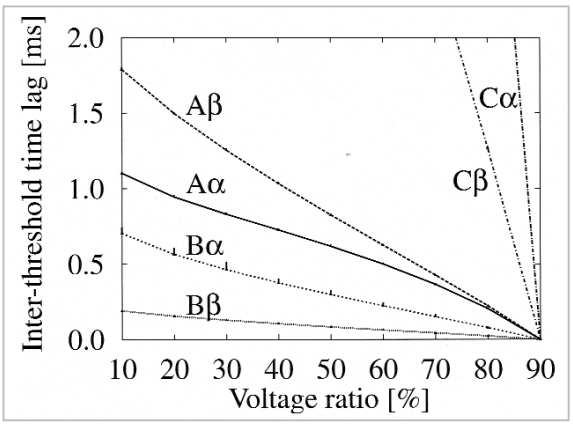

Fig.8 *Averaged time-lag-normalized voltage relationships for all models*

mitters of the same model and manufacturer. The possibility of this last identification will be described in view of time-frequency space in another report[5].

3 Experiment using an antenna

We conducted an experiment using an antenna by changing conditions such as the receiver input intensity level, S/N ratio, IF bandwidth, and trigger point. To eliminate as many variables as possible and improve reliability, one common receiver antenna and one common transmitter antenna were installed. They were separated by approximately 300 meters to prevent the effect of box radiation. No hindrance, such as tall building, was present between them.

Fig. 9 shows the discone antenna that was available on the market and installed on a building (Building No.3) rooftop. An attenuator was placed between the antenna and transmitter to adjust the output power to that required by the receiver. A stabilized power supply was used for the transmitters, and they were examined under the same conditions as in the indoor experiment. Appendix 1 shows a list of the transmitters tested in the indoor experiment. The circled transmitters in this list were tested in the present experiment.

Fig. 9 *Discone antenna for use in the present experiment*

3.1 Data acquisition through an antenna

In the experiment using an antenna to acquire data, it was likely that data acquisition was affected by interference and a lowered S/N ratio caused by neighboring radio stations in the same band. We first studied these effects on transmitter identification. Fig.10 shows a measured amplitude waveform that was affected by such interference and noise. A 145-MHz FM transceiver, TR51 of Manufacturer i, was used under conditions in which Att of 30 dB was added to a transmission output of 5 W, the receiver input-level Pin was –110 dBm, and the S/N ratio was 7.2 dB.

Fig.11 shows an amplitude waveform obtained in the indoor experiment. A comparison of Figs. 10 and 11 revealed that data acquired through an antenna contained a large amount of noise, and that the distorted signals made it difficult to obtain the characteristics at the rise of a waveform. Fig.12 shows a spectrogram obtained by using fast Fourier transformation (FFT) to convert I-Q data into a frequency region. Fig.13 shows a spectrogram for the indoor experiment obtained by using FFT to convert the field-experiment I-Q data into a frequency region.

In Fig.10, the waveform seems to have been affected greatly by noise. However, it proved to be interference that actually affected the waveform. As can be seen in Fig.12, the raw data can be separated into the signal, interference-induced wave, and noise. The effect on the waveform depended on the degree of interference. A comparison between the waveform and interference by overlaying revealed no deformation or distortion of the spectrogram. This will be described in greater detail in the figure of a spectrogram pattern shown below. Unlike in the indoor experiment, waveform data acquired through an antenna proved to be useless for identifying transmitters unless noise and interference were sufficiently negligible. On the other hand, very little effect was seen on the spectrogram

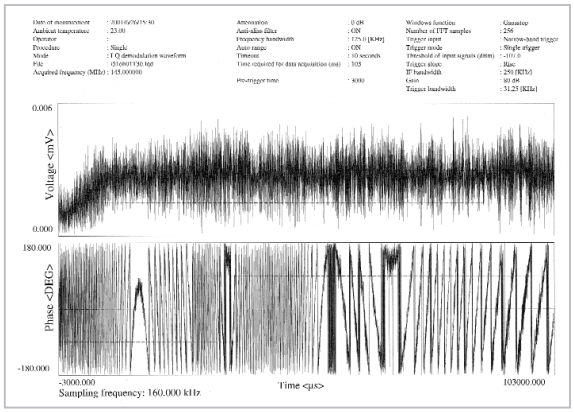

Fig.10 *Measured amplitude waveform affected by interference on Tr51*

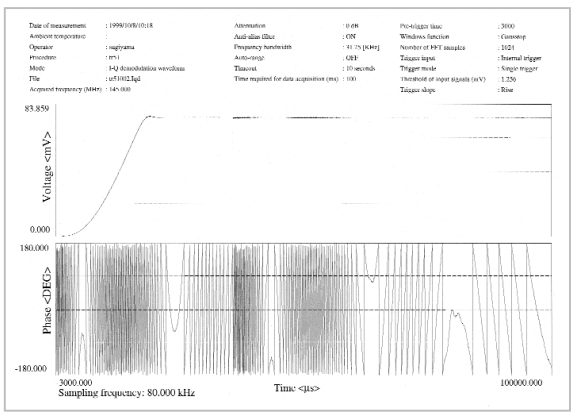

Fig.11 *Amplitude waveform obtained in the indoor experiment using Tr51*

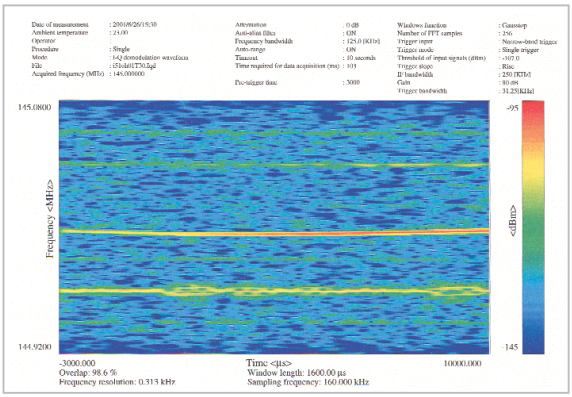

Fig.12 *Spectrogram affected by interference on Tr51*

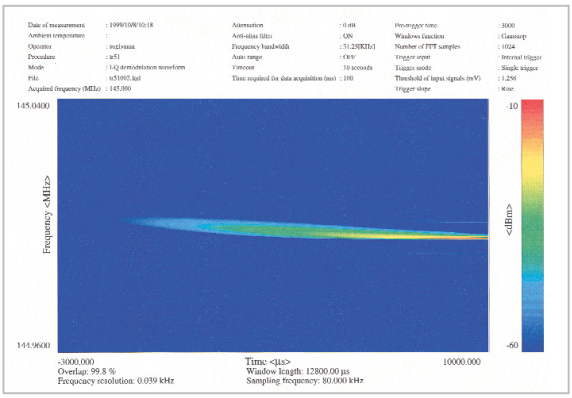

Fig.13 *Spectrogram obtained in the indoor experiment using Tr51*

calculated from the data acquired through an antenna. The pattern of a spectrogram proved to be useful for identifying transmitters in both the indoor experiment and field antenna experiment. The next section will describe the usefulness of the spectrogram pattern.

3.2 Data processing

The previous section discussed the capability of a spectrogram obtained by converting I-Q data through FFT. This application software enables determination of the frequency and spectrum intensity at any point specified using a mouse cursor. When this function is used, the displayable range of the screen is 10 ms. In this study, to obtain the entire pattern of the spectrogram, we moved the cursor to the peak spectrum every 1 ms in order to read the frequency and spectrum intensity.

Fig.14 shows the frequency (upper) and spectrum intensity (lower) obtained for transceiver Tr51 of Manufacturer i. The attenuation level for transmission was 0 dB, 10 dB, 20 dB, and 30 dB. The frequency gradually changed with the attenuation level, up to 20 dB. With 30-dB attenuation, the pattern shifted forward significantly. Now we will explain the results of the examination about the trigger setting and the shifted pattern. The indoor experiment confirmed that this type of transmitter produced by Manufacturer i caused a frequency step of between 20 ms and 40 ms. For attenuation of 0 dB, Fig.14 indicates that frequency stepping took place 33 ms after the trigger started. In this figure, ① through ④ indicate the occurrence of frequency stepping when the input-level Pin was switched using the attenuator. For ① through ③, the stepping was small and shifted forward by approximately 2 ms. For ③ and ④, the stepping shifted by 5 ms. It should be noted that the trigger setting was unchanged between 0 dB and 20 dB, while at 30 dB it was changed by –97 dBm to –107 dBm. The entire patterns shifted due to the effects of a change in the trigger setting and the lowered S/N ratio. These effects did not result in distortion of the pattern.

Fig.14 (lower) shows the dependencies of the peak of a spectrum signal on the elapsed time. The signal level increased slowly following a rise for a duration of over ten ms, and then became constant. Switching of the attenuator every 10 dB caused an expected change in the signal level. This confirmed that the equipment and related software operated normally.

Fig.15 shows the time at which stepping took place for the four transmitters at a trigger level of 0 dBm based on the results of the indoor experiment. For Tr51, all data points are plotted.

Next, we examined transmitter Tr39 of Manufacturer y, as it showed a large frequency change at the time of a rise, and the change was not reproducible in a number of measurements. Fig.16 shows the averages and errors for the peak frequency with an interval of 1 ms, in ten measurements that were taken during the first 40 ms after a rise. This figure

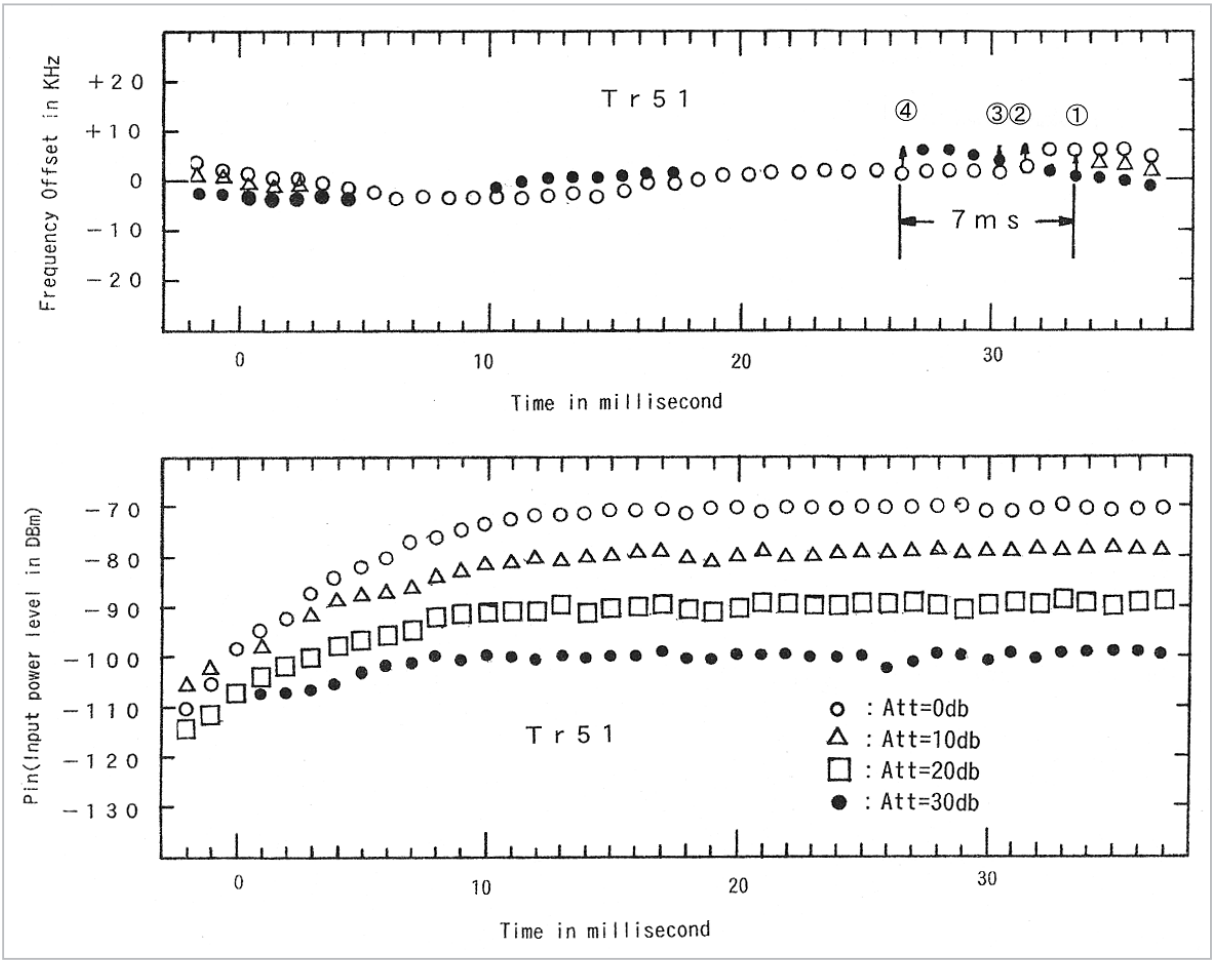

Fig.14 *Frequency (upper) and spectrum intensity (lower) with an interval of 10 ms for transceiver Tr51 of Manufacturer i*

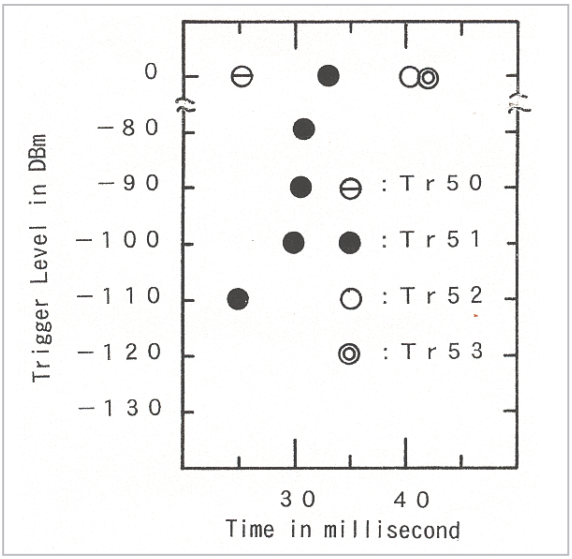

Fig.15 *Time at which stepping occurred for the four transmitters at a trigger level of 0 dBm. For Tr51 of Manufacturer i, all data points are plotted*

indicates that approximately 16 ms were required for the peak frequency to stabilize following convergence. As the attenuation increased from 0 dB to 30 dB, the peak-frequency average peaked earlier. As with Tr51, this was an effect of the trigger-level setting. As can also be seen in this figure, the average did not lie in the center of the error bar.

Fig.17 shows the results for four transmitters of the same model. When data overlaps as shown in this figure, it is difficult to identify the transmitters. This is a problem that remains to be solved in the future.

Fig.18 shows the results obtained in a field experiment in which Att = 10 dB (◯) and in an indoor experiment (●). The indoor-experiment result is the average of measurements of the peak frequency. The arrows indicate fluctuations. The average peak frequency was similar in the two experiments, while the time of occurrence of the peak frequency in the

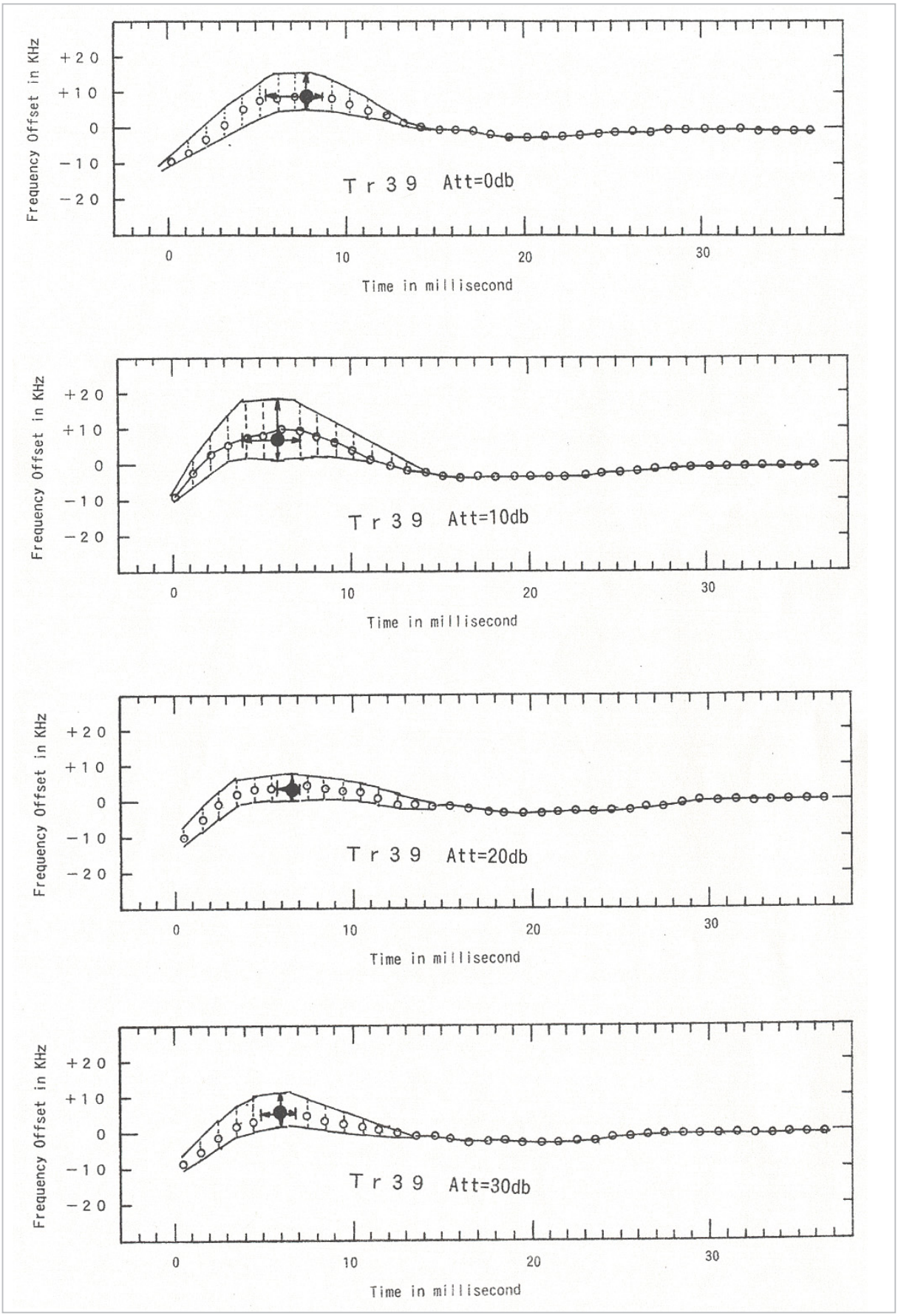

Fig.16 *Averages and errors for the peak frequency with an interval of 10 ms for transmitter Tr39 of Manufacturer y*

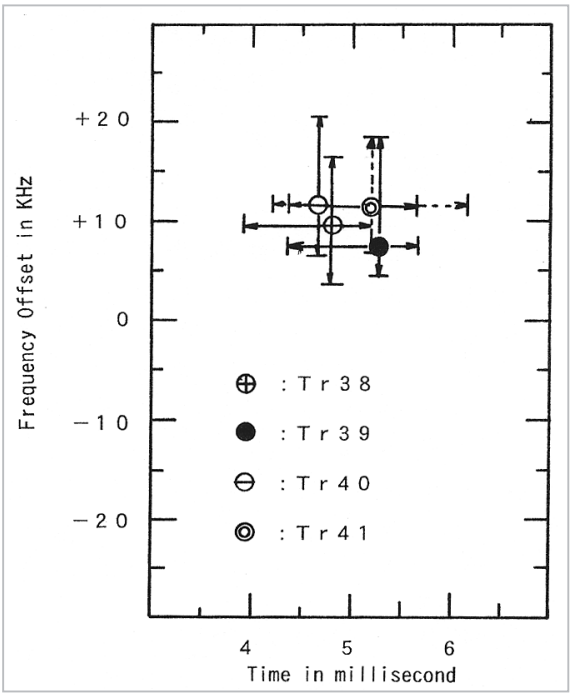

Fig.17 *Time at which a frequency peak occurred for four transmitters of Tr39 of Manufacturer y*

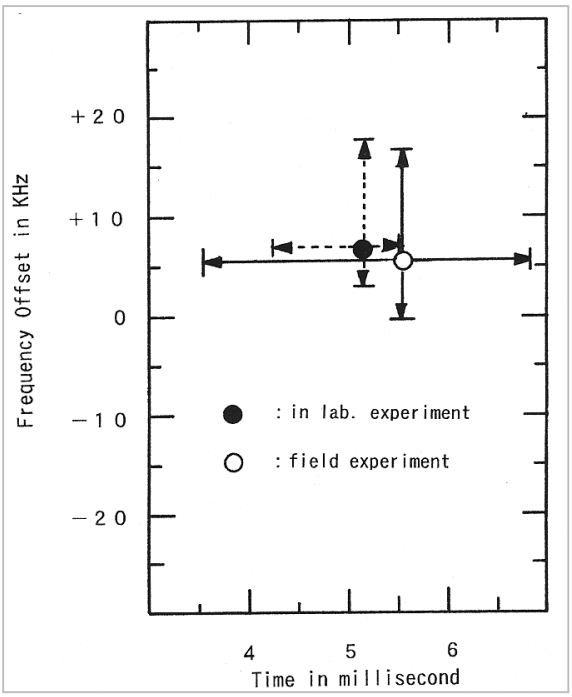

Fig.18 *Comparison of the time at which a frequency peak occurred in a field experiment and indoor experiment*

field experiment showed fluctuations twice that seen in the indoor experiment. This is due to the fact that the receiver functions using the antenna produced noise that seemed to have an adverse effect on data.

4 Spectrogram pattern

Acquired data was converted into a spectrogram. A spectrogram pattern was used to identify the adequate features of the transmitter. A pattern such as that obtained using a 10-ms interval in the previous section was not sufficient to identify the transmitter. We needed a tool that would enable the quick and accurate acquisition of a spectrogram pattern. For this purpose, we applied software developed in the course of analyzing data.

Fig.19 shows an example obtained using the above software. The upper graph shows the absolute values of amplitude. To obtain the lower graph, fast Fourier transformation (FFT) was first applied to the raw data with a data length (Nfft) of 1024 bits in order to obtain a spectrogram. The lower graph in Fig.19 shows the contours of this spectrogram, with an interval of 0.05% between 10% and 95% of the peak level (Pmax). The contours correspond to decibel steps down to –22 dB, with step intervals being between 1 dB and 2 dB. The data length of 1024 bits was selected in consideration of the frequency resolution, time resolution, and spectrum density distribution. The vertical axis in the lower graph indicates the deviation from the center frequency within a range of ±15 kHz. The horizontal axis indicates the elapsed time from the start of triggering to 102 ms. This tool enables the selection of a linear scale (as shown in this graph) or decibel scale. This graph clearly confirms the frequency step characteristics of transmitter Tr51 in the spectrogram pattern.

Fig.20 shows an example, similar to that shown in Fig.19, in which attenuation of 30 dB was applied to create strong interference. While Fig.19 indicates only small effects of interference and noise on the raw amplitude data, Fig.20 indicates that the effects of interference and noise are too large to confirm the original waveform. As shown in Fig.14, the change in the trigger settings and the S/N ratio (from 24.3 dB to 7.2 dB) caused the entire spectrogram pattern to shift backward by approximately 4 μs. The spectrogram patterns

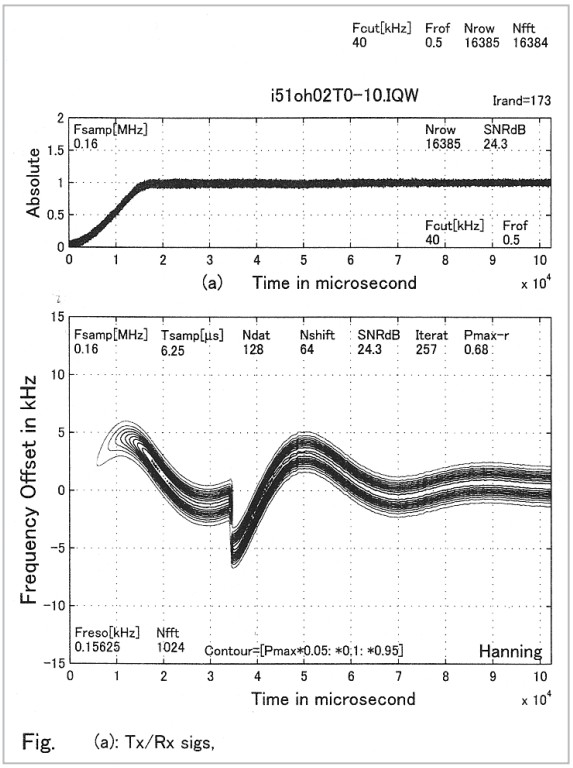

Fig. (a): Tx/Rx sigs,

Fig.19 *Amplitude waveform and calculated spectrogram pattern for transmitter Tr51*

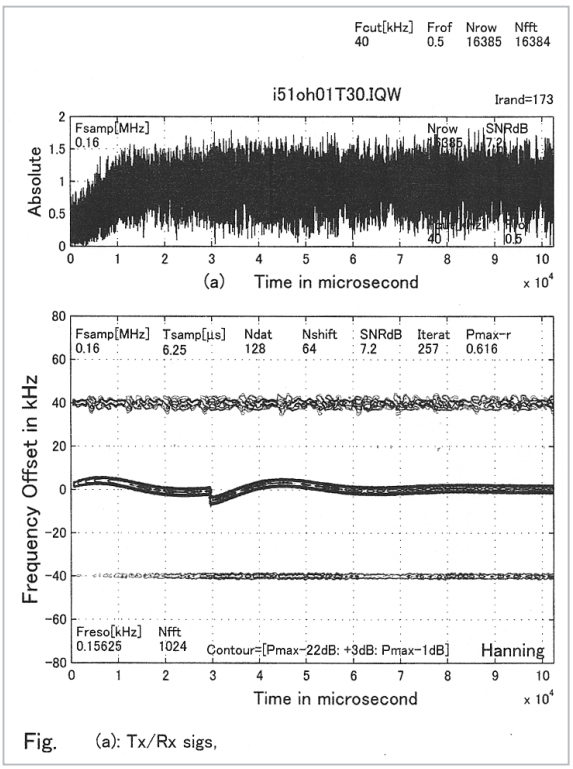

Fig. (a): Tx/Rx sigs,

Fig.20 *Amplitude waveform and calculated spectrogram pattern affected by attenuation of 30 dB to create strong interference*

shown in Figs. 14 and 20 were examined and found to be in good agreement without significant distortion.

Fig. 21 and 22 show the calculated spectrogram patterns for transmitter Tr39 of Manufacturer y. This transmitter experienced a steep change in frequency in the initial period (0 to 30 ms) after a rise. Thereafter, the frequency converged quickly to the set value. The graphs in these figures contain calculations of the largest and smallest changes in frequency in ten measurements. As shown in Fig.17, four transmitters of the same type as Tr39 produced very similar characteristics for frequency stepping. As this data overlaps closely, it was impossible to identify the transmitters. This is a problem that remains to be solved in the future.

Fig.23 shows the calculated spectrogram patterns for transmitter Tr32 of Manufacturer k. This transmitter experienced a steep change in frequency in the initial period after a rise, followed by an oscillatory attenuation. Other transmitters produced complex patterns and were identifiable.

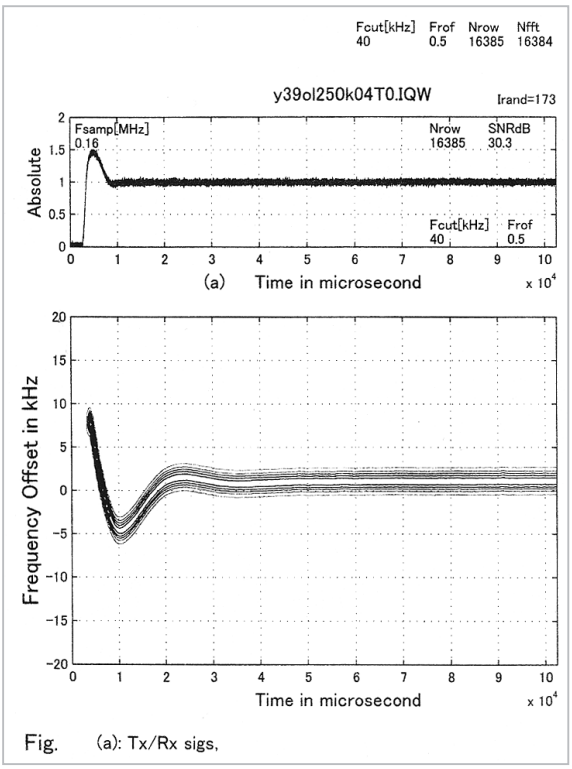

Fig. (a): Tx/Rx sigs,

Fig.21 *Calculated spectrogram patterns (1) for transmitter Tr39*

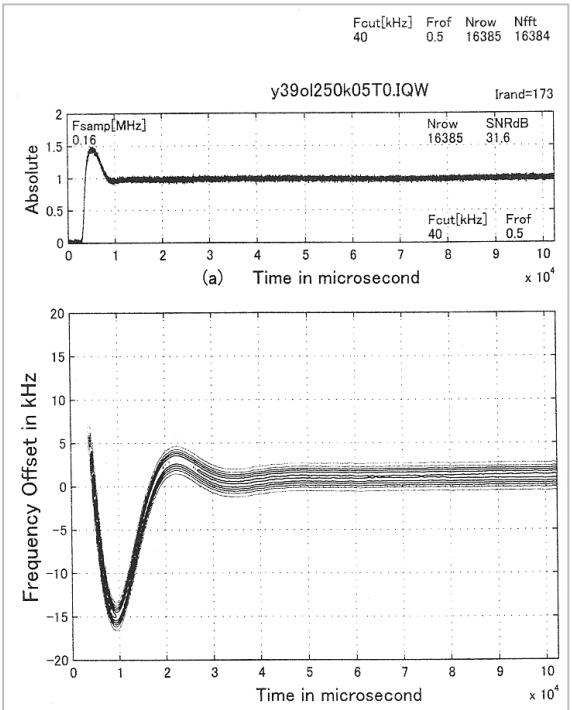

Fig. (a): Tx/Rx sigs,

Fig.22 *Calculated spectrogram patterns (2) for transmitter Tr39*

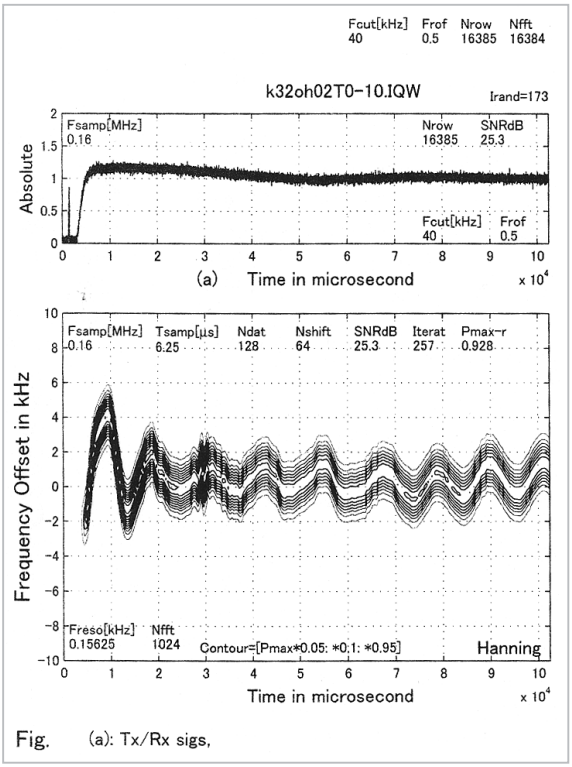

Fig. (a): Tx/Rx sigs,

Fig.23 *Calculated spectrogram patterns for transmitter Tr32*

5 Spectrogram pattern and IF bandwidth

All measurements described in the preceding sections were made with the IF bandwidth fixed at 250 kHz. A low-pass filter for 40 kHz was applied to produce absolute values of amplified waveform and spectrogram patterns. In this section, we describe the IF bandwidth and the low-pass filter.

Fig.24 shows the spectrogram pattern obtained by applying a low-pass filter with a cutoff frequency of 20 kHz to the I-Q data measured with an IF bandwidth of 50 kHz by transmitter Tr39 of Manufacturer y. In Figs. 21 and 22, which were obtained using the same transmitter, Tr39, the amplitude waveform initially overshot and then maintained a constant level. In Fig.24, the initial portion showed distortion due to the effect of the low-pass filter for eliminating frequencies above the cutoff value. However, the spectrogram pattern was not affected.

Fig.25 shows a spectrogram pattern obtained by applying a low-pass filter with a cutoff frequency of 10 kHz to the I-Q data measured with an IF bandwidth of 12 kHz by transmitter Tr39 of Manufacturer y. The initial portion of the amplitude waveform showed much larger distortion than in Fig.24. However, the spectrogram pattern was not affected, except for lack of data above the cutoff value due to the filter. The transmitter was still identifiable.

As the bandwidth decreases, noise is reduced, thereby improving the S/N ratio. This may result in a loss of information contained in signals, and in significant distortion of amplitude waveforms. On the other hand, spectrogram patterns are not distorted, but lack only the above cutoff value. Otherwise, the patterns are the same as the original patterns. Therefore, even under conditions in which noise has a large effect, the processing of signals using a low-pass filter to a narrower bandwidth should be effective in the identification of transmitters.

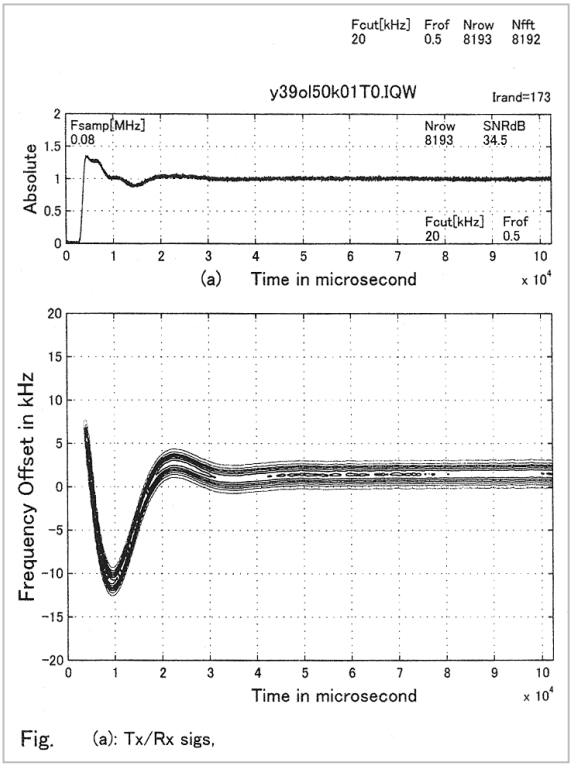

Fig.24 *Spectrogram pattern obtained by applying a low-pass filter with an IF bandwidth of 50 kHz using transmitter Tr39*

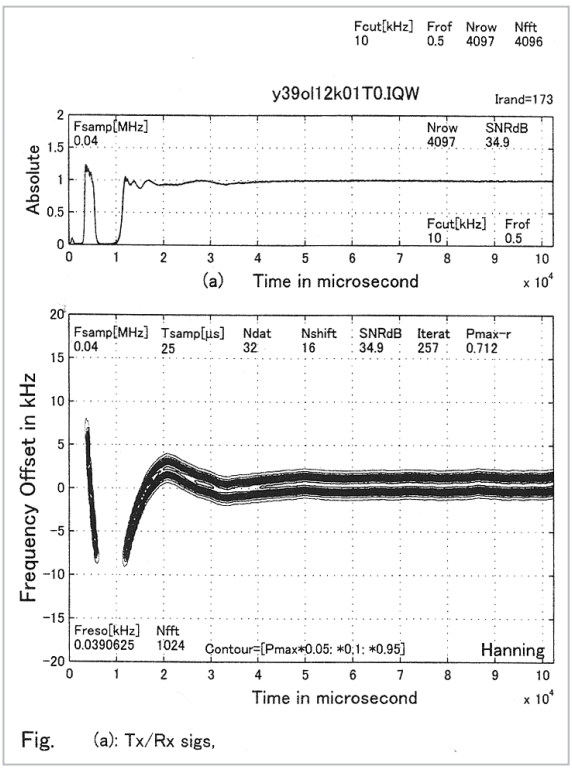

Fig.25 *Spectrogram pattern obtained by applying a low-pass filter with an IF bandwidth of 12 kHz using transmitter Tr39*

6 Wigner distribution

We first applied Wigner distributions to identify transmitters, as the use of fast Fourier transformation (FFT) provides good resolutions of frequency and time. In this report, we applied spectrogram patterns using FFT. Although a Wigner distribution features a resolution of frequency twice that of a spectrogram pattern, no significant difference was reported in previous studies between calculations of different sources[6]. Although the distributions produce good instant frequency expression over time, they are directly affected by noise and interference. Thus, we decided to apply spectrogram patterns using FFT to identify transmitters. We found that the selection of an adequate data length enabled such identification without lowering the resolutions of frequency and time.

Fig.26 shows a spectrogram calculated with a data length of Nfft of 128 bits. The resolutions of frequency and time in this spectrogram are approximately one-eighth and eight times, respectively, of those in a spectrogram obtained with a data length of Nfft of 1024 bits. These large differences resulted in a loss of smoothness in the entire region containing large frequency fluctuations. By changing the data length, we found a length of Nfft of 1024 bits to be most adequate in the analysis of amplitude waveforms. We therefore decided to use a data length of Nfft of 1024 bits in this study.

Fig.27 shows a spectrogram pattern for a logarithmic scale. Fig.28 shows the Wigner distribution of the same data for a logarithmic scale. These figures indicate that effects of both noise and the spectrum width differed between the two types of calculations. The Wigner distribution was better in terms of the frequency resolution, was influenced more by noises, and had a narrower spectrum bandwidth. The basic patterns are the same in the two modes, making them suitable for the identification of transmitters. For details on the procedure and evaluation of these analytical techniques, refer to a technical manual.

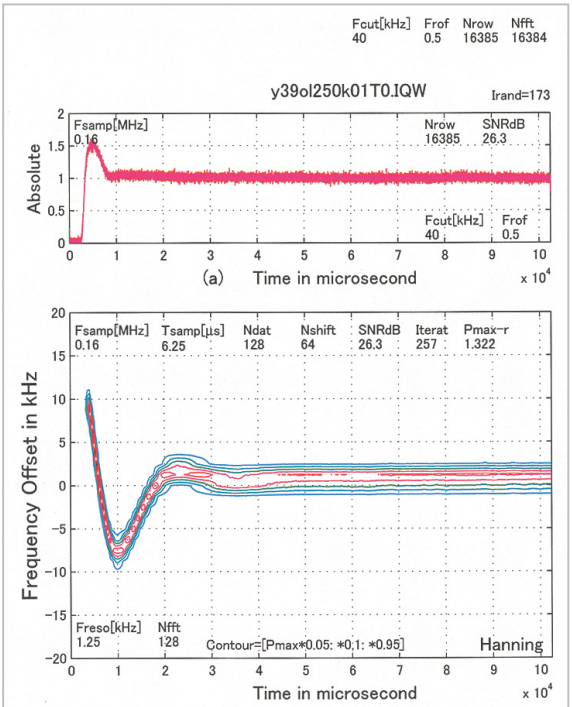

Fig. (a): Tx/Rx sigs,

Fig.26 *Amplified waveform and spectrogram pattern calculated with a data length of Nfft of 128 bits*

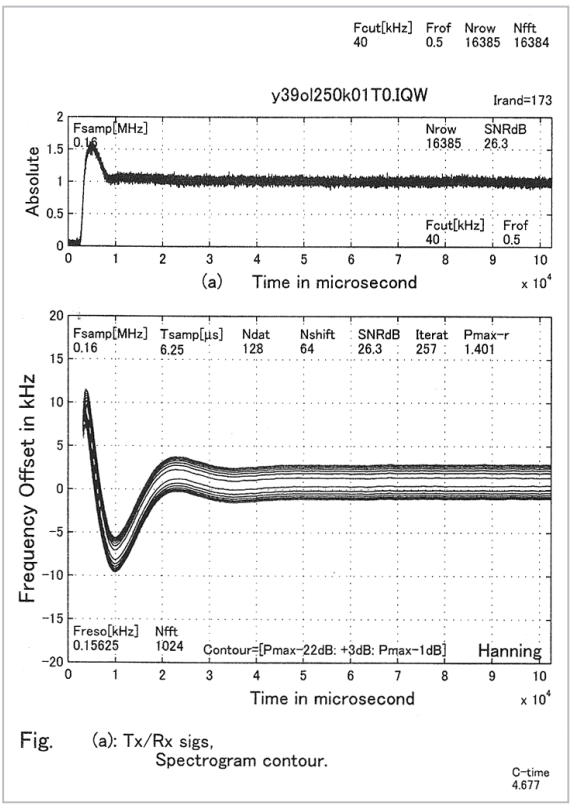

Fig. (a): Tx/Rx sigs,
Spectrogram contour.
C-time
4.677

Fig.27 *Amplified waveform and spectrogram pattern calculated with a data length of Nfft of 1024 bits*

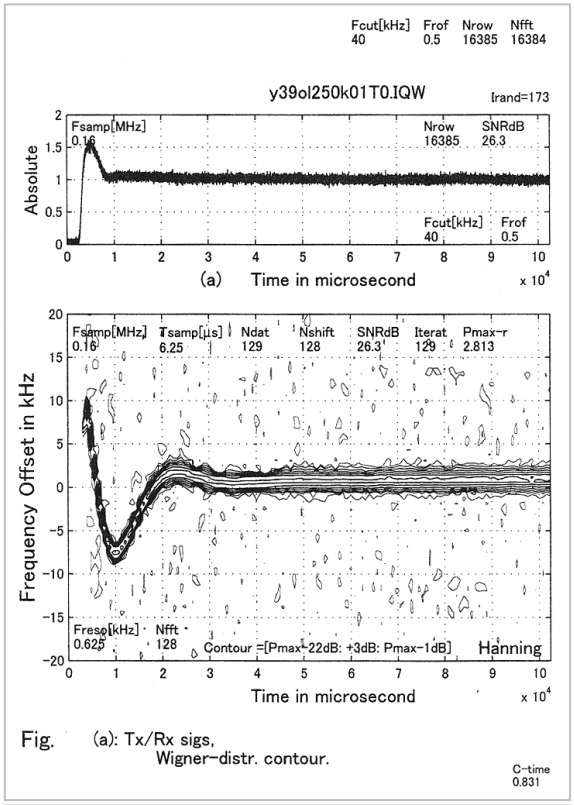

Fig. (a): Tx/Rx sigs,
Wigner-distr. contour.
C-time
0.831

Fig.28 *Amplified waveform and spectrogram pattern obtained using a Wigner distribution*

7 Conclusions

Using a high-speed data-acquisition system with a receiving function, we examined the effects of the receiver input-level conversion (Pin) on envelope waveforms and spectrogram patterns at the time of a time-domain rise. As the Pin lowered, the S/N ratio also lowered due to the external noise. This lowering was compared with the results obtained in an indoor experiment in which there was no interference with neighboring radio stations. It was found that the waveforms in the time domain were too distorted for the identification of transmitters. On the other hand, it was found that original signals, noise, and interference waves were separated in spectrograms. Furthermore, the control of a bandwidth using a filter had no effects on the portions of the spectrogram pattern outside the cutoff time range. Thus, spectrogram patterns proved to be effective in identifying transmitters. It should be noted that they were capable of

identifying types of transmitters, but that individual transmitters of the same type were not always identifiable because some of them have almost the same spectrogram patterns. This latter fact is a problem that remains to be solved in the future.

Acknowledgements

The present study was conducted with the financial support of the Ministry of Posts and Telecommunications (currently the Ministry of Public Management, Home Affairs, and Posts and Telecommunications). We would like to express our gratitude for the assistance provided by those at the Ministry and the Communications Research Laboratory. We would also like to express our thanks to Mr. Yasuo Suzuki and Mr. Yoshitada Kato of Agilent Technologies for their help in the development of the data-acquisition system. In addition, we wish to thank Mr. Chihiro Miki, Senior Researcher, for his help with the application of a radio station. Finally, thanks to Mr. Shunkichi Isobe, Leader of the Scientific Technology Information Group, for his valuable advice prior to publication.

References

1 Radio Use Website, http://www.tele.soumu.go.jp/e/

2 Y.Ichino, A.Suzuki, T.Sugiyama and M.Kamata, "Application of Wigner-Ville Distribution of Radio Equipment Identification", IEICE Trans. B-Ⅱ, Vol.J77-B-Ⅱ, No.10, pp.584-586, Oct. 1994 (in Japanese).

3 W.Shiobara, N.Ojima, R.Chino and T.Takahashi, "Transient variation in the transmitter frequency of a mobile FM transmitter when its press-to-talk switch is operated", Review of the Radio Research Laboratory, Vol.17, No.90, pp.281-286, May 1971 (in Japanese).

4 T.Sugiyama, M.Shibuki, T.Hirano, K.Iwasaki, "Data Acquisition System and Radio Transmitter Rising Envelope on Radio Transmitter Identification", Proc. IEICE General Conf., B-4-23, Mar. 2000 (in Japanese).

5 T.Hirano, T.Sugiyama, M.Shibuki and K.Iwasaki, "Study on Time-Frequency Spectrum Pattern for Radio Transmitter Identification", Proc. IEICE General Conf., B-4-24, Mar. 2000 (in Japanese).

6 K.Iwasaki, T.Hirano, M.Shibuki and T.Sugiyama, "A Data Analysis Method for Radio Transmitter Identification Based on Transient Response -Root-MUSIC Method-", Research discourse meeting, May 1999 (in Japanese).

Appendix 1 Specifications for the transmitters tested in the present study

N	Manufacturer	Type	Frequency	Output	Model number	Serial number	Remarks
30	KENWOOD	TH-42	430MHz	5W/13.8V	KU071-35002	00700052	Aβ1
31		TH-42	430MHz	5W/13.8V	KU071-35003	00700053	○Aβ2
32		TH-42	430MHz	5W/13.8V	KU071-35004	00700054	Aβ3
33		TH-42	430MHz	5W/13.8V	KU071-35947	01100077	Aβ4
34	KENWOOD	TH-22	144MHz	5W/13.8V	KV070-22017	91200127	Aα1
35		TH-22	144MHz	5W/13.8V	KV070-22326	00100176	Aα2
36		TH-22	144MHz	5W/13.8V	KV070-22825	00400275	Aα3
37		TH-22	144MHz	5W/13.8V	KV070-24234	01200094	Aα4
38	YAESU	FT-40N	430MHz	5W/12V	KU167-04935	9D230035	Bβ1
39		FT-40N	430MHz	5W/12V	KU167-04936	9D230036	○Bβ2
40		FT-40N	430MHz	5W/12V	KU167-04937	9D230037	Bβ3
41		FT-40N	430MHz	5W/12V	KU167-04938	9D230038	Bβ4
42	YAESU	FT-10N	144MHz	5W/12V	KV166-03191	8I190091	Bα1
43		FT-10N	144MHz	5W/12V	KV166-03192	8I190092	Bα2
44		FT-10N	144MHz	5W/12V	KV166-03198	8I190098	Bα3
45		FT-10N	144MHz	5W/12V	KV199-98023	8J066004	Bα4
46	ICOM	IC-T32	430MHz	5W/13.5V	KU153-03881	03881	Cβ1
47		IC-T32	430MHz	5W/13.5V	KU153-04637	04637	○Cβ2
48		IC-T32	430MHz	5W/13.5V	KU153-05556	05556	Cβ3
49		IC-T32	430MHz	5W/13.5V	KU153-05711	05711	Cβ4
50	ICOM	IC-T22	144MHz	5W/13.5V	KV152-02552	02552	Cα1
51		IC-T22	144MHz	5W/13.5V	KV152-02556	02556	○Cα2
52		IC-T22	144MHz	5W/13.5V	KV152-03346	03346	Cα3
53		IC-T22	144MHz	5W/13.5V	KV152-03354	03354	Cα4

The symbols given in the Remarks section indicate the names used in this report.
A circle indicates a transmitter tested in the field experiment.

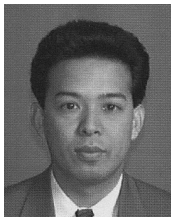

Tsutomu SUGIYAMA

Researcher, Radio and Measurement Technology Group, Applied Research and Standards Division

Development of type approval test

Masaaki SHIBUKI

Senior Researcher, Radio and Measurement Technology Group, Applied Research and Standards Division

Standard Time and Frequency

Ken IWASAKI

Senior Researcher, Radio and Measurement Technology Group, Applied Research and Standards Division

Mobile Communications

Takayuki HIRANO

STA fellowship